

ORIGINAL ARTICLE

Correspondence:

Sung Won Lee, Department of Urology, Samsung Medical Center, Samsung Biomedical Research Institute, Sungkyunkwan University School of Medicine, 81 Irwon-ro, Gangnam-gu, Seoul 06351, Korea.
E-mail: drswlee@skku.edu

Keywords:

Hv1 channel, onion (*Allium cepa* L.) peel extract, quercetin, sperm motility



Received: 29-Sep-2016

Revised: 13-Jun-2017

Accepted: 27-Jun-2017

doi: 10.1111/andr.12406

Onion (*Allium cepa* L.) peel extract (OPE) regulates human sperm motility via protein kinase C-mediated activation of the human voltage-gated proton channel

¹M. R. Chae, ¹S. J. Kang, ²K. P. Lee, ³B. R. Choi, ⁴H. K. Kim, ³J. K. Park ,
⁵C. Y. Kim and ¹S. W. Lee 

¹Department of Urology, Samsung Medical Center, Samsung Biomedical Research Institute, Sungkyunkwan University School of Medicine, Seoul, Korea, ²Laboratory of Physiology, College of Veterinary Medicine, Chungnam National University, Daejeon, Korea, ³Department of Urology, Medical School and Institute for Medical Sciences, Chonbuk National University, Research Institute and Clinical Trial Center of Medical Device of Chonbuk National University Hospital, Jeonju, Korea, ⁴College of Pharmacy, Kyungshin University, Busan, Korea, and ⁵College of Pharmacy and Institute of Pharmaceutical Science and Technology, Hanyang University, Ansan, Korea

SUMMARY

Onion (*Allium cepa* L.) and quercetin protect against oxidative damage and have positive effects on multiple functional parameters of spermatozoa, including viability and motility. However, the associated underlying mechanisms of action have not yet been identified. The aim of this study was to investigate the effect of onion peel extract (OPE) on voltage-gated proton (Hv1) channels, which play a critical role in rapid proton extrusion. This process underlies a wide range of physiological processes, particularly male fertility. The whole-cell patch-clamp technique was used to record the changes in Hv1 currents in HEK293 cells transiently transfected with human Hv1 (HVCN1). The effects of OPE on human sperm motility were also analyzed. OPE significantly activated the outward-rectifying proton currents in a concentration-dependent manner, with an EC₅₀ value of 30 µg/mL. This effect was largely reversible upon washout. Moreover, OPE induced an increase in the proton current amplitude and decreased the time constant of activation at 0 mV from 4.9 ± 1.7 to 0.6 ± 0.1 sec ($n = 6$). In the presence of OPE, the half-activation voltage ($V_{1/2}$) shifted in the negative direction, from 20.1 ± 5.8 to 5.2 ± 8.7 mV ($n = 6$), but the slope was not significantly altered. The OPE-induced current was profoundly inhibited by 10 µM Zn²⁺, the most potent Hv1 channel inhibitor, and was also inhibited by treatment with GF109203X, a specific protein kinase C (PKC) inhibitor. Furthermore, sperm motility was significantly increased in the OPE-treated groups. OPE exhibits protective effects on sperm motility, at least partially via regulation of the proton channel. Moreover, similar effects were exerted by quercetin, the major flavonoid in OPE. These results suggest OPE, which is rich in the potent Hv1 channel activator quercetin, as a possible new candidate treatment for human infertility.

INTRODUCTION

Infertility affects approximately 10–15% of all couples of reproductive age, and approximately 45–50% of all infertility cases are due to male infertility (Farhi & Ben-Haroush, 2011; Hamada *et al.*, 2012). The single most common cause of male infertility is defective sperm function. However, in 30–40% of such cases, the reason for sperm dysfunction has not yet been identified. Thus, there is no specific therapy or effective treatment for idiopathic cases of infertility.

For the last decade, successful recording of the ionic currents from mature spermatozoa has identified the primary ion channels in spermatozoa. These ion channels play a central role in sperm physiology and the process of fertilization by controlling intracellular pH, membrane potential, and intracellular Ca²⁺. In addition, loss of functional ion channels could cause male infertility without affecting other physiological functions (Kirichok & Lishko, 2011; Lishko *et al.*, 2012). The intracellular pH of spermatozoa is a major regulator of motility, capacitation,

hyperactivation, and the acrosome reaction in the female reproductive tract (Koch *et al.*, 2008). More specifically, the human voltage-gated proton (Hv1) channel has an indispensable role in male fertility because it allows rapid and effective proton conductance, thereby activating the Ca^{2+} permeable sperm cation channel (Lishko *et al.*, 2010).

Voltage-gated proton channels are expressed in many cell types, including phagocytes, neurons, airway epithelial cells, muscle cells, and spermatozoa (Decoursey, 2003; Okochi *et al.*, 2009; Iovannisci *et al.*, 2010; Lishko *et al.*, 2010). These channels play critical roles in host defense (Ramsey *et al.*, 2009), sperm capacitance (Lishko *et al.*, 2010), and motility (Musset *et al.*, 2012), and cancer metastasis (Wang *et al.*, 2012). Hv1 channels are highly selective for protons and are controlled by changes in the transmembrane voltage and pH gradient.

In humans, Hv1 channels are highly expressed in spermatozoa and have been proposed to play a vital role in the regulation of intracellular pH (Lishko *et al.*, 2010). Moreover, reduced expression of Hv1 has been reported in patients with infertility and teratozoospermia (Platts *et al.*, 2007). Hv1 channel activation in alkaline seminal fluid or in the female reproductive tract results in proton extrusion, leading to intracellular alkalization and spermatozoa activation (Lishko *et al.*, 2010). Intraflagellar alkalization via the Hv1 channel consequently activates the CatSper channel (Kirichok *et al.*, 2006), a sperm-specific Ca^{2+} channel, which co-localizes with the Hv1 channel within the principal piece of the sperm flagellum. These events increase the intracellular calcium concentration in spermatozoa, thereby changing the flagellar beat pattern to vigorous, high-amplitude asymmetric flagellar beating. This pattern is known as hyperactivation and is mediated by a Ca^{2+} -sensing protein called calaxin. This hyperactive motility is necessary for spermatozoa to penetrate the zona pellucida and fertilize the egg. Thus, the regulation of intracellular pH and cytosolic free Ca^{2+} concentration via the combined action of the Hv1 and CatSper channels is crucial for many physiological processes of spermatozoa, including motility, capacitation, and the acrosome reaction in the female reproductive tract.

Onion (*Allium cepa* L.) has been widely used in traditional folk medicine since ancient times and is known to exert various biological functions via its hypocholesterolemic, thrombolytic, anti-asthmatic, and antioxidant effects (Lanzotti, 2006). In particular, quercetin, the most abundant flavonoid in onion peel, has been identified as a potent antioxidant.

Although many studies have shown that onion and quercetin protect against oxidative damage and have positive effects on multiple functional parameters of spermatozoa, including viability and motility (Izawa *et al.*, 2008; Ola-Mudathir *et al.*, 2008; Khaki *et al.*, 2009; Saber *et al.*, 2016), the mechanisms underlying these effects have not yet been identified.

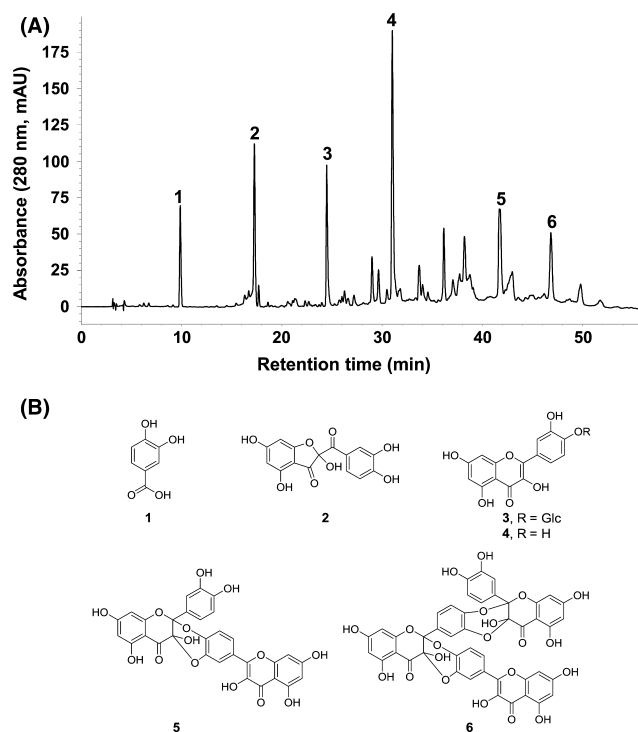
In this study, we investigated the effects of onion peel extract (OPE) and quercetin on the activity of Hv1 channels. We also examined the mechanism responsible for these effects in HEK293 cells expressing Hv1 channels.

MATERIALS AND METHODS

Preparation of crude extract

Onion was purchased from the local market, and the brown outer layers were extracted three times with ethanol under reflux

Figure 1 HPLC chromatogram of onion extract (A) and its major constituent compounds (B). Compounds (1–6) were identified using HPLC-ESI/MS. Peak identification: protocatechuic acid (1), 2-(3,4-dihydroxybenzoyl)-2,4,6-trihydroxy-3(2H)-benzofuranone (2), quercetin 4'-O- β -D-glucopyranoside (3), quercetin (4), 1,3,11a-trihydroxy-9-(3,5,7-trihydroxy-4H-1-benzopyran-4-on-2-yl)-5a-(3,4-dihydroxyphenyl)-5,6,11-hexahydro-5,6,11-trioxanaphthacene-12-one (5, quercetin dimer), and 1,3,11a-trihydroxy-9-(3,5,7-trihydroxy-4H-1-benzopyran-4-on-2-yl)-5a-[1,3,11a-trihydroxy-5a-(3,4-dihydroxyphenyl)-5,6,11-hexahydro-5,6,11-trioxanaphthacene-12-on-9-yl]-5,6,11-hexahydro-5,6,11-trioxanaphthacene-12-one (6, quercetin trimer).



for 3 h. The combined filtrate was concentrated using a rotary evaporator, freeze dried, and stored at -20°C until further analyzes. The crude extract was analyzed using HPLC. Here, 10 mg of crude extract was dissolved in 1 mL of methanol and filtered through a $0.45\ \mu\text{m}$ membrane filter. To identify the major constituents of the onion extract, $5\ \mu\text{L}$ of the filtrate was injected onto an INNO C18 column ($2.0\ \text{mm} \times 150\ \text{mm}$, Younglin Biochrom, Seoul, South Korea) in an HPLC-ESI/MS system. The system consisted of an Agilent 1260 HPLC system (Agilent Technologies, Waldbronn, Germany) equipped with an Advion Expression CMS mass spectrometer (Advion, NY, USA). The HPLC profile of the onion extract and the compounds identified from it are shown in Fig. 1. Peaks were identified by matching the recorded HPLC retention times with those of previously reported mass data (Ly *et al.*, 2005).

Cell culture and transfection

The human embryonic kidney cell line HEK293 was purchased from the American Type Culture Collection (Manassas, VA, USA). Cells were maintained in Dulbecco's modified Eagle's medium (DMEM, Life Technologies, Carlsbad, CA, USA) supplemented with 10% fetal bovine serum and antibiotics (100 units/mL penicillin, streptomycin; Gibco). Cells were cultured in a 5% CO_2 atmosphere. For transfection, HEK293 cells were seeded into 12-well plates at a density of 10^5 cells/well and grown for

24 h. The cells were transiently transfected with pQBI25-FC3-GFP, which encodes human Hv1 (HVCN1) and was kindly provided by Dr. David Clapham and Dr. Scott Ramsey. All transfections were performed using Lipofectamine® 3000 (Life Technologies). At 20–24 h after transfection, the cells were used in electrophysiological experiments. The expression of green fluorescent protein (GFP)-fusion proteins was detected using an IX 70 inverted fluorescence microscope (Eclipse Ti-U, Nikon, Tokyo, Japan).

Electrophysiological recordings

Electrophysiological recordings were performed in a whole-cell patch-clamp configuration using an Axopatch-200B amplifier and a Digidata 1440A instrument (Molecular Devices, Sunnyvale, CA, USA). The patch-clamp pipettes were made from filament-containing borosilicate glass capillary tubing (World Precision Instruments, Sarasota, FL, USA) and pulled using a Narishige PP-830 vertical puller (Narishige Group, Tokyo, Japan). Next, the tip was heat-polished using a microforge MF-830 (Narishige Group) to obtain a resistance of 3–5 MΩ when filled with the indicated pipette solutions. The reference electrode was an Ag-AgCl wire connected to the bath solution through a 3 M KCl-agar bridge. To record the Hv1 currents, the cell suspension was placed into a small chamber (0.6 mL) on the stage of an inverted fluorescence microscope (Nikon). Next, seals were formed with normal Tyrode's solution (in mM: 135 NaCl, 5 KCl, 10 HEPES, 1.8 CaCl₂, 1 MgCl₂, and 10 glucose, pH 7.4), and the pipettes were filled with the following solution (in mM): 65 N-methyl-D-glucamine, 3 MgCl₂, 1 EGTA, 70 glucose and 100 MES (pH 6.0 with CH₃SO₃H). The bath solution for the recording contained the following (in mM): 75 N-methyl-D-glucamine, 1 CaCl₂, 1 MgCl₂, 10 glucose, and 100 HEPES (pH 7.0–7.8 with CH₃SO₃H). All measurements were performed at room temperature (22–25 °C). The current traces were sampled at 5 kHz and filtered at 1 kHz. The data were analyzed using CLAMPFIT 9.2 (Molecular Devices) and ORIGIN 8.0 (OriginLab, Northampton, MA, USA) software. The current densities were calculated by normalizing the current amplitudes to the membrane capacitances.

Conductance-voltage (G-V) plots were fitted with the Boltzmann equation ($G/G_{\max} = 1/[1 + \exp((V_{1/2} - V)/S)]$), where $V_{1/2}$ is the half-activation potential, V is the membrane potential, S is the slope factor, and G_{\max} is the slope conductance.

OPE, Compounds 1 and 3, and quercetin were dissolved in dimethyl sulfoxide (DMSO) to form stock solutions. GF109203X was also dissolved in DMSO. The final concentration of DMSO was <0.1% and did not affect the membrane currents. To evaluate the concentration-dependent effect of OPE on the Hv1 currents, serial dilutions were prepared by diluting 200 mg/mL OPE stocks and then adding to the bath solution at concentrations ranging from 1 to 200 μg/mL. Compounds 1 and 3 and quercetin were prepared by diluting 100 mM stock solutions in bath solution at the desired final concentrations immediately before use. The cells were treated in bath solution containing various concentrations of OPE (1, 10, 25, 50, 100, 200 μg/mL) or quercetin (1, 10, 30, 100, 200 μM). To evaluate whether protein kinase C (PKC) was involved in the OPE- or quercetin-induced potentiation of the Hv1 channels, the cells were treated with the PKC inhibitor

GF109203X (3 μM, extracellular) after stimulation with 100 μg/mL OPE or 200 μM quercetin.

Quercetin, GF109203X, and all other chemicals were purchased from Sigma Chemical (St. Louis, MO, USA).

Sperm motility

All study materials were reviewed and approved by the Institutional Review Board of Chonbuk National University Hospital (CUH 2012-03-001-008). As participants for our study, we identified male patients who visited our hospital for urological evaluations from January 2015 to December 2015. The inclusion criteria were sperm count $\geq 20 \times 10^6$ /mL and sperm motility $\geq 40\%$. All sperm tests were performed according to the WHO recommendations. Written informed consent was obtained from all subjects before study enrollment. This study was conducted in accordance with the International Conference on Harmonization Good Clinical Practice guidelines and in conformity with the ethical principles of the declaration of Helsinki. Samples were collected from participants following abstinence from ejaculation for a minimum of 72 h and no longer than 7 days before collection. All specimens were obtained by masturbation without using a condom and were maintained in an incubator at room temperature for 1 h at 37 °C.

Sperm motility was evaluated by observing the sperm suspension within 3–5 min after being placed in the counting chamber (Makler/Sperm Meter, Product Code: Sperm Counting Chamber; SEFI-Medical Instruments LTD, New York, NY, USA); this method mitigates error due to the tendency of spermatozoa to migrate from the periphery. Motile spermatozoa within the 10 center squares of the grid were counted under a light microscope (Axio Imager 2, UMD Code: 393099; Carl Zeiss Microimaging LLC, Goettingen, Germany), and mean sperm counts were recorded. Sperm counts were also measured 3 h after incubation with OPE. The percentage of motile spermatozoa was determined by the following formula: (mean number of motile spermatozoa/total number of spermatozoa) $\times 100$. All counts were performed at 37 °C in Ham's F-10 medium (0.4% HAS, 12 mM HEPES).

The total sperm count was calculated using two or three drops of specimen to increase the reliability of the count. The counting chamber is composed of two parts: The upper part is a cover glass encircled with a metal ring. At the center of its lower surface, there is a 1 mm² grid that is subdivided into 100 squares of 0.1 \times 0.1 mm. When the cover glass is placed on the four tips, the volume bounded in a row of 10 squares is exactly one-millionth of 1 mL. Therefore, the number of sperm heads in 10 squares indicates their concentration in million/mL. We measured the sperm count of 10 center squares of the grid counted under a light microscope and included existing spermatozoa in the 10 center squares. The increase in sperm motility was determined by the following formula: increase (%) = [(Sperm motility after 3 h of incubation – Sperm motility after 0 h of incubation)/Sperm motility after 3 h of incubation] $\times 100$.

Statistical analysis

All data are expressed as the mean \pm SEM; n refers to the number of cells examined. The Wilcoxon signed rank test was employed to compare group mean values. Differences were considered significant if $p < 0.05$.

RESULTS

Identification of the Hv1 channel

To characterize the Hv1 channels, we measured the proton currents from HEK293 cells expressing human Hv1 protein using whole-cell patch-clamp recording. Figure 2 shows the slowly activating outward currents in response to depolarizing pulses; these currents were both voltage-dependent and pH-dependent. As is characteristic of Hv1, increasing extracellular pH (pH_o) increased the current amplitude and the threshold for current activation (Fig. 2A,B). The reversal potential is one of the most important parameters of ion channel selectivity (Hille, 1986). To assess the reversal potential, we used the tail current protocol, in which the conductance is initiated by the application of depolarizing pulses (+80 mV for 2 sec) followed by deactivating pulses

to potentials ranging from +20 mV to −100 mV. Under the conditions used (pipette pH 6.0), the reversal potentials (V_{rev}) at the pH_o values of 7.0, 7.4, and 7.8 were −24, −63, and −71 mV, respectively. However, the equilibrium potentials calculated from the Nernst equation ($E_{\text{H}} = -58 \cdot \log([H]_o/[H]_i)$) are −58, −81.2, and −104.4 mV at pH_o 7.0, 7.4, and 7.8, respectively. Although the measured reversal potentials deviated from the calculated potentials, the measured reversal potential shifted in response to the H^+ gradient as external pH increased (Fig. 2C).

Activation effect of OPE on the Hv1 channel

To assess the effect of OPE on voltage-dependent proton channels, proton currents were recorded in the presence of 50 $\mu\text{g/mL}$ OPE by applying ramp pulses from −80 to 100 mV from a holding potential of −60 mV at 30 sec intervals. At an

Figure 2 Effects of altering external pH on current. HEK293 cells were transfected with GFP only (Aa, Ba) or with HVCN1 (Ab, Bb). (A) Currents were measured under different extracellular pH conditions (pH_i 6.0; pH_o 7.0, 7.4, 7.8) using 10-mV steps from −60 to +100 mV. The holding potential was −60 mV. (B) Current–voltage relationships obtained using a 2-sec ramp pulse from −80 to +100 mV. (C) pH dependence of average V_{rev} (\pm SEM, $n = 6$) determined by tail currents. To record the tail current, the membrane was depolarized pre-pulse to +80 mV for 2 sec, followed by repolarization to between −100 and +20 mV.

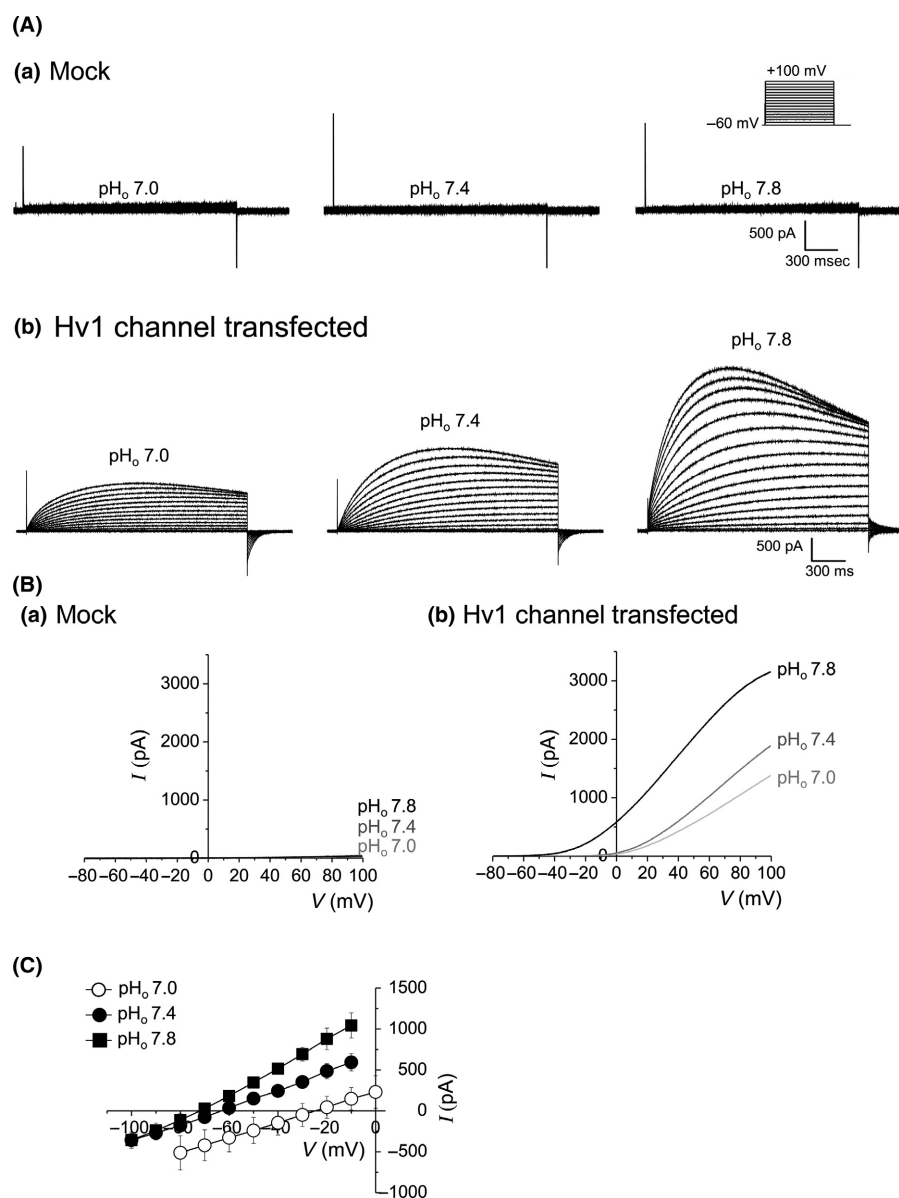
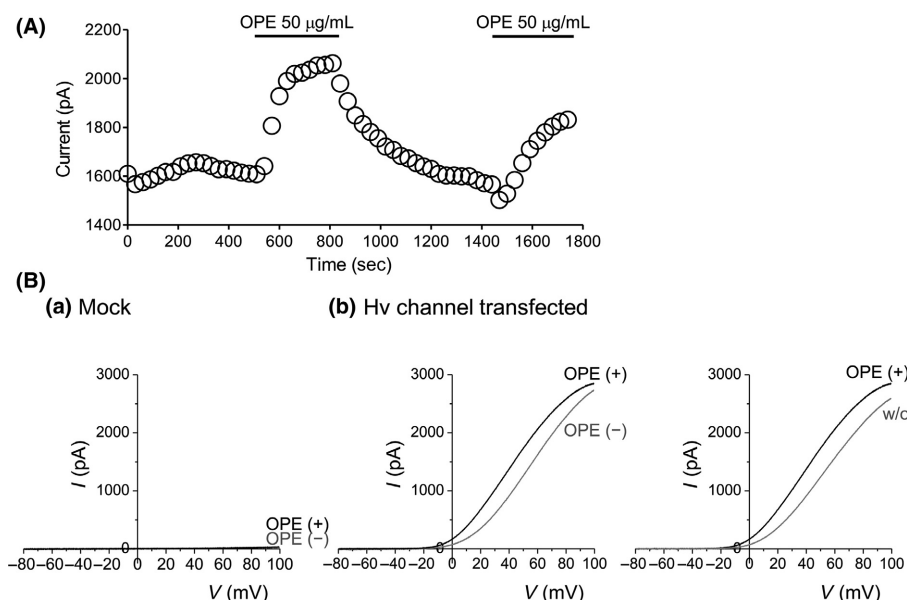


Figure 3 OPE-activated Hv1 currents. (A) Representative sustained currents obtained at +60 mV from HEK293 cells expressing Hv1 (pipette pH_i 6.0, bath pH_o 7.4). The holding potential was −60 mV. Currents were measured before and after the addition of 50 μg/mL OPE, after which cells were washed with bath solution. (B) Current–voltage relationships were obtained from a mock-transfected cell (Ba) and from an Hv1-transfected cell (Bb) using a 2-sec ramp pulse from −80 to +100 mV.



intracellular/extracellular pH gradient of 6.0/7.4, the extracellular addition of OPE (50 μg/mL) caused a significant increase in the outward currents (Fig. 3A). Following washout using the bath solution, the channel currents returned to basal levels. Repeated application of OPE produced approximately 70% of the current amplitude of the first application. OPE activated outward-rectifying proton currents and shifted the current–voltage (*I*–*V*) relation curves to the left (Fig. 3B). However, this effect was not observed in non-transfected HEK293 cells. Thus, these results indicate that OPE reversibly potentiates Hv1 channel activity.

Concentration-dependent effect of OPE on the Hv1 channel

As shown in the current traces in Fig. 4A, the activation of proton currents by OPE was concentration dependent. At the maximum concentration tested (200 μg/mL), this effect was largely reversible upon washout. Figure 4 (panels B and C) shows the *I*–*V* curves obtained after the application and washout of OPE. OPE progressively shifted the *I*–*V* curves to the left in a dose-dependent manner. Figure 4D summarizes the average values at +60 mV, showing that the current density gradually increased as the OPE concentration increased. Concentrations above 25 μg/mL had significant effects on Hv1 channels. The amplitudes of the OPE-evoked responses were similar for 100 and 200 μg/mL, suggesting that 100 μg/mL was the saturation point. Thus, we used 100 μg/mL OPE in all subsequent experiments. The dose–response curve is shown in Fig. 4E. The normalized currents were plotted against the OPE concentration on a semi-log scale. The best fit using the Hill equation was a continuous line between the data points. The EC₅₀ and Hill coefficient values were 30 μg/mL and 1.5, respectively.

OPE affects the gating properties of Hv1 channels

To define the mechanism of OPE-induced Hv1 channel activation, we investigated the effect of OPE on activation kinetics. As

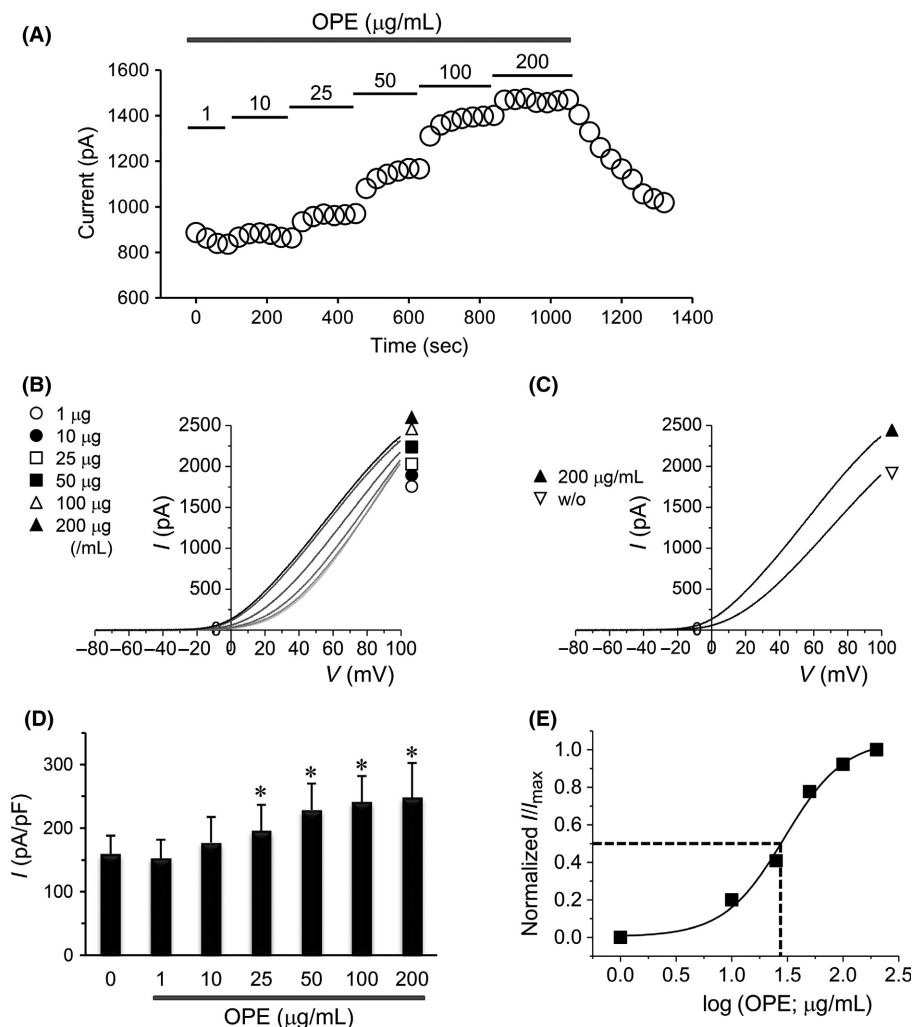
shown in Fig. 5A, Hv1 currents evoked by 100 μg/mL OPE were activated much more quickly than the control currents. The activation time constant was significantly decreased, from 4.9 ± 1.7 to 0.6 ± 0.1 sec at 0 mV ($n = 6$, $p < 0.05$), after OPE treatment (Fig. 5B). To determine the effect of OPE on the voltage dependence of the channel activation, the relative conductance (G/G_{\max}) was obtained by normalizing the tail currents that were fitted using the Boltzmann equation. As shown in Fig. 5C, the *G*–*V* relationships showed voltage-dependent activation of proton currents and were shifted in the negative direction by the addition of 100 μg/mL OPE. Moreover, the half-activation voltage ($V_{1/2}$) shifted approximately 15 mV, from 20.1 ± 5.8 mV to 5.2 ± 8.7 mV ($n = 6$, $p < 0.05$). However, the slope was not significantly altered by OPE treatment. Thus, these results demonstrate that OPE potentiates the activity of the Hv1 channel by modulating channel opening and activating the channel at negative membrane voltages.

To confirm whether the currents stimulated by OPE result from Hv1 channel activation, we assessed the effect of Zn²⁺, a classical inhibitor of Hv1 channels, on OPE-stimulated currents. The addition of 10 μM ZnCl₂ profoundly inhibited the OPE-induced currents, slowing activation and shifting the *g*H–*V* relationship in the positive direction (Fig. 6), as has been observed in other cells (Cherny & DeCoursey, 1999).

Effect of the PKC inhibitor GF109203X on OPE-mediated stimulation of Hv1 channels

The enhanced gating mode of the proton channel is elicited by protein kinase C (PKC)-dependent phosphorylation. Thus, to determine the potential contribution of the phosphorylation status of the Hv1 channel to these OPE-mediated effects, the effects of the PKC-specific inhibitor GF109203X were assessed in OPE-treated cells. As shown in Fig. 7, the addition of 3 μM GF109203X subsequent to OPE abolished the effects of OPE. In the presence of GF109203X, the OPE-enhanced proton current was greatly

Figure 4 Concentration-dependent activation of Hv1 currents by OPE. (A) Representative current traces obtained at +60 mV in the presence of various concentrations of OPE. Horizontal lines indicate the application of OPE. OPE was applied at 1–200 $\mu\text{g/mL}$ to Hv1-overexpressing HEK293 cells. $\text{pH}_i = 6.0$; $\text{pH}_o = 7.4$. (B) Maximum current–voltage relationships were obtained before (control) and after the addition of various concentrations of OPE. All currents were induced by a ramp protocol from -80 to $+100$ mV for 2 sec. (C) Current–voltage relationships after washing with bath solution. (D) Summary of the dose-dependent increase in Hv1 current in response to the addition of OPE at +60 mV. Bars represent mean \pm SEM. $*p < 0.05$ vs. control cells (0 $\mu\text{g/mL}$) ($n = 9$). (E) Dose-response curves for OPE activation of Hv1 currents. Peak currents activated were normalized to the control value. Mean values were fitted using the Hill equation.



reduced. Furthermore, this effect was largely reversible upon drug washout.

Effect of OPE on sperm motility

The effects of OPE on the motility of spermatozoa from human semen samples are shown in Table 1. The samples observed after 3 h of incubation with OPE (50 $\mu\text{g/mL}$) showed greater sperm motility than the control group. For patient 2, the sperm motility changed from 50.0% (after 0 h of incubation with Ham's F-10 medium) to 49.0% (after 3 h of incubation with Ham's F-10 medium) in the control group and increased from 45.7% (after 0 h of incubation with OPE) to 65.2% (after 3 h of incubation with OPE) in the OPE group.

Effects of Compounds 1 and 3 and quercetin on the Hv1 channel

To identify the main active components of OPE, we evaluated the proton currents after treatment with quercetin or with

Compound 1 or Compound 3, two of the six compounds identified from OPE. Figure 8 shows the representative I – V curves obtained after the extracellular application of Compound 1, Compound 3, or quercetin. The application of 100 μM Compound 1 for 10 min had no effect on Hv1 channel currents. In contrast, Compound 3 at the same concentration increased Hv1 currents within a few minutes. Moreover, subsequent addition of quercetin to the same cells did not evoke much larger currents than those induced by Compound 3. Figure 8B summarizes the average values at +60 mV, showing that the mean current density induced by Compound 3 was not significantly different from that induced by quercetin (at 60 mV, control: 134.0 ± 27.1 pA/pF, Compound 1: 124.0 ± 21.0 pA/pF, Compound 3: 171.3 ± 35.6 pA/pF, quercetin: 173.4 ± 36.1 , $n = 6$).

To further investigate the effect of quercetin, increasing concentrations of quercetin were applied to the extracellular sides of membrane patches. As shown in the I – V curves in Fig. 9A, quercetin increased the current in a concentration-dependent

Figure 5 Effect of OPE on the voltage dependence of Hv1 current activation. (A) Representative superimposed current trace obtained in response to 2 sec depolarizing steps to potentials between -60 to $+100$ mV in 10 mV increments applied from a holding potential of -60 mV. $pH_i = 6.0$; $pH_o = 7.4$. (B) Activation time constants of Hv1 currents. The time constants were determined from single exponential fits to the rising current phases. The activation time constants were voltage-dependent and were decreased after OPE treatment. The data are expressed as the mean \pm SEM ($n = 8$). (C) Relative conductance vs. voltage ($(G/G_{max}) - V$) curves. Curves were obtained from experimental tail current measurements, such as those shown in A. The data were fitted using the Boltzmann function. Each point represents the mean \pm SEM ($n = 8$).

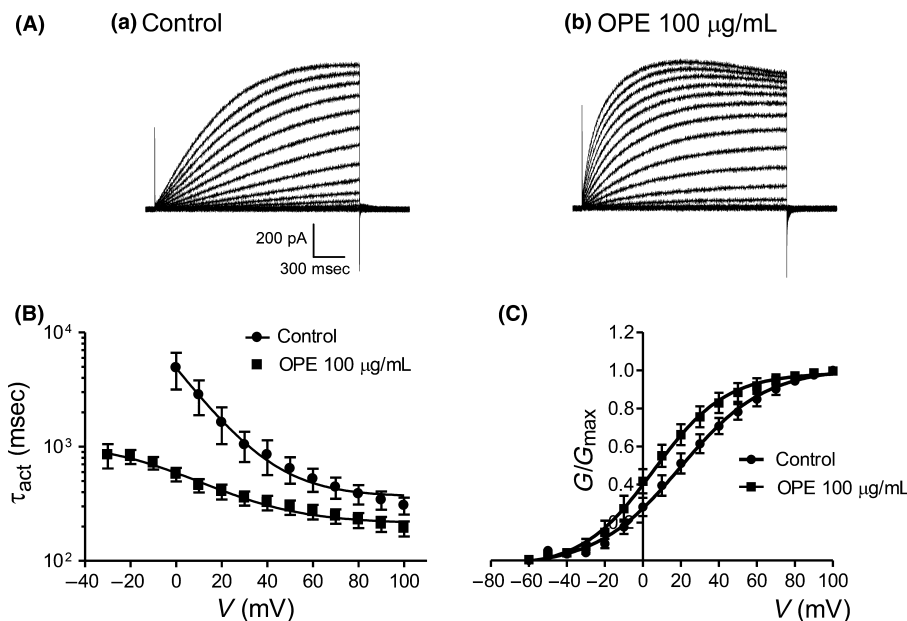
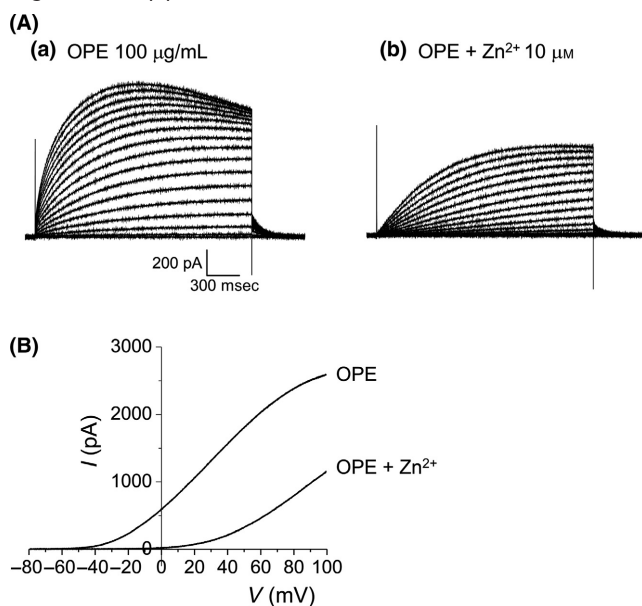


Figure 6 Effect of Zn^{2+} on OPE-induced outward currents. (A) Representative superimposed currents evoked by voltage steps (-60 to $+100$ mV in 10 -mV increments) were recorded in the presence of 100 µg/mL OPE or OPE plus 10 µM Zn^{2+} . $pH_i = 6.0$; $pH_o = 7.4$. OPE-activated current was inhibited by 10 µM Zn^{2+} ($n = 8$). (B) Current-voltage relationships obtained using a 2-sec ramp pulse from -80 to $+100$ mV.



manner. Quercetin-induced increases in current plateaued at approximately 100 µM; the currents then rapidly returned to the pretreatment level after drug washout (data not shown). Figure 9B summarizes the average values at $+60$ mV. The EC_{50} of quercetin for the Hv1 channel was calculated as 30 µM. Similar

to its effect on OPE, application of 3 µM GF109203X also reduced the quercetin-enhanced proton currents ($n = 5$, $p < 0.05$) (Fig. 9C). The similarity of the responses elicited by OPE and quercetin indicates that quercetin functions as a major active component in the OPE-induced enhancement of Hv1 channel activity.

DISCUSSION

In the present study, we found that OPE significantly potentiates Hv1 channel currents in a dose-dependent manner, with an EC_{50} value of 30 µg/mL. OPE induced the enhanced gating mode of the proton channel, decreased the time constant of activation, and shifted the $G-V$ relationship toward the negative. This current potentiation was profoundly inhibited by the addition of 10 µM Zn^{2+} , the most potent known Hv1 channel inhibitor. We also observed that the specific PKC inhibitor GF109203X reversed these effects of OPE. OPE increases human sperm motility. In addition to OPE, we also evaluated the effects of Compound 1, Compound 3, and quercetin on Hv1 channel currents. Compound 3 and quercetin increased the proton currents with almost the same potency, while compound 1 did not affect proton currents. Quercetin significantly potentiates Hv1 channel currents in a dose-dependent manner, yielding EC_{50} values of 30 µM. Similar to its effect on OPE, GF109203X reduced the quercetin-enhanced proton current.

Voltage-gated proton channels are highly selective for H^+ and closely follow the Nernst equation for permeability. The tail current protocol provided the deviated reversal potentials from the predicted H^+ equilibrium potentials. These deviations could occur when large I_H carries H^+ out of cells and might have increased the internal pH (pH_i). To avoid deviation of reversal potentials from predicted H^+ equilibrium potentials, TE

Figure 7 Effect of GF109203X on enhanced Hv1 channel gating by OPE. (A) Representative current traces recorded in the presence of 100 $\mu\text{g/mL}$ OPE and after applying 3 μM GF109203X. Current–voltage relationships were obtained in (A) at the points indicated by the arrows with small letters (a–c). Currents were recorded by a ramp protocol from -80 to $+100$ mV for 2 sec in control cells and after the addition of 100 $\mu\text{g/mL}$ OPE (a) and 3 μM GF109203X (b). $\text{pH}_i = 6.0$ and $\text{pH}_o = 7.4$. (B) Summary of peak current densities at $+90$ mV. Bars represent the mean \pm SEM. $*p < 0.05$ vs. control cells ($n = 7$). GFX: GF109203X.

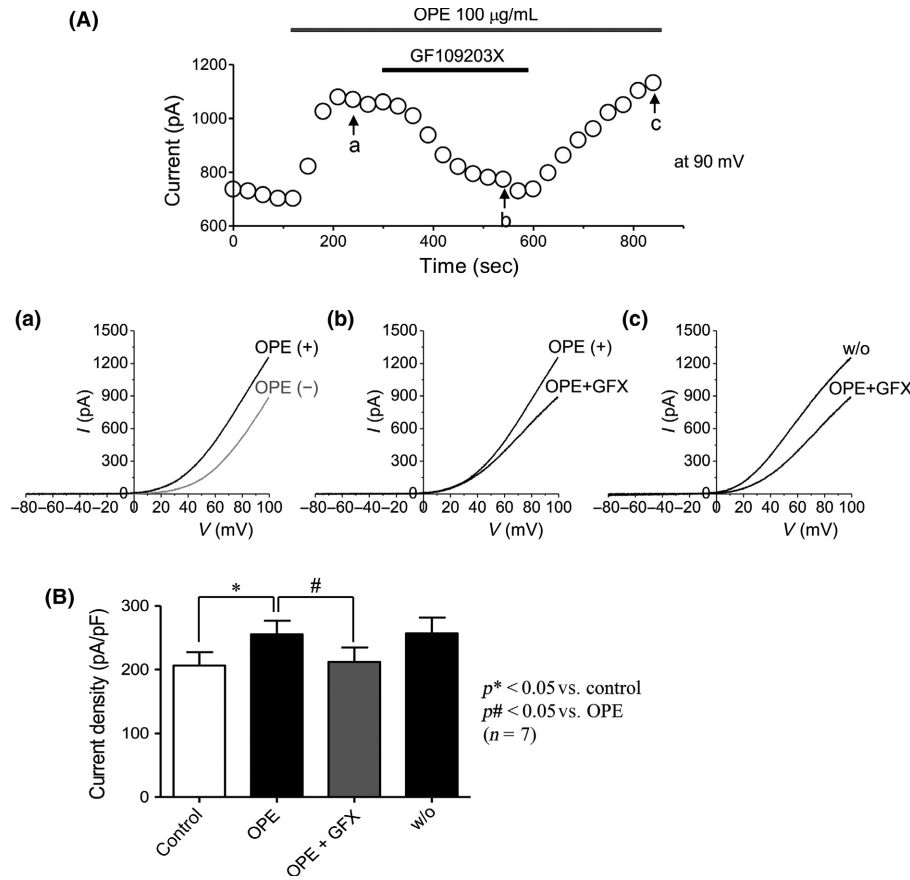


Table 1 Effect of OPE on sperm motility

Group		Zero		3 h		Increase in sperm motility (%)
		Count ($10^6/\text{mL}$)	Motility (%)	Count ($10^6/\text{mL}$)	Motility (%)	
Patient 1	Control	59	54.6	56	54.0	–1.11
	OPE 50 $\mu\text{g/mL}$	56	55.7	51	66.0	17.27
Patient 2	Control	63	50.0	47	49.0	–2.04
	OPE 50 $\mu\text{g/mL}$	61	45.7	52	65.2	23.31
Patient 3	Control	53	54.0	58	51.7	–4.45
	OPE 50 $\mu\text{g/mL}$	53	54.1	48	60.5	10.74
Patient 4	Control	37	47.0	33	40.0	–17.50
	OPE 50 $\mu\text{g/mL}$	26	47.1	30	56.6	16.96
Patient 5	Control	45	60.0	49	57.6	–4.17
	OPE 50 $\mu\text{g/mL}$	58	57.7	54	63.8	5.96
Patient 6	Control	43	57.2	32	55.3	–3.44
	OPE 50 $\mu\text{g/mL}$	46	59.1	38	64.0	10.63

DeCoursey tested whether higher buffer concentration in the pipette solution minimized the distortion due to H^+ depletion. In his experiments, the V_{rev} in experiments with higher buffer

concentration (119 mM MES) was closer to E_{H} than when a lower buffer concentration (5 mM MES) was used DeCoursey, (1991). Therefore, the current experimental buffer concentration (100 mM MES) was not able to completely prevent the increase in pH_i , and an altered V_{rev} was observed.

Onion peel has a high quercetin content. The quercetin in onion peel is present in one of the following conjugated forms: quercetin 4'-O- β -glycopyranoside, quercetin 3,4'-O- β -diglycopyranoside, or quercetin 3,7,4'-O- β -triglycopyranoside. Recently, several clinical and animal studies have demonstrated that onion peel exhibits a wide range of biological activities, such as antioxidative, anticarcinogenic, and anti-inflammatory properties (Jung *et al.*, 2011; Lee *et al.*, 2012; Moon *et al.*, 2013; Kim & Yim, 2015). The bioactivity of quercetin could be attributed to its specific molecular structure. Specifically, quercetin has five OH groups, phenolic hydroxyls, and a 2,3-unsaturated double bond. The bioactivity of quercetin includes powerful antioxidant properties and oxyradical scavenging activity due to its ability to interact with and penetrate lipid bilayers. In addition to its antioxidant activity, quercetin also has pro-oxidant properties under certain circumstances (Prochazkova *et al.*, 2011). Quercetin has been shown to increase the levels of H_2O_2 , superoxide anion radicals and lipid peroxidation products in a concentration-dependent manner (Yen *et al.*, 2003). H_2O_2 production

Figure 8 Effects of Compounds 1 and 2 and quercetin on Hv1 currents. (A) Typical current–voltage relationships were obtained using a 2-sec ramp pulse from -80 to $+100$ mV. Membrane currents were recorded 10 min after application of Compound 1 (○), Compound 3 (●) or quercetin (□), each at $100\ \mu\text{M}$. $\text{pH}_i = 6.0$ and $\text{pH}_o = 7.4$. (B) Summary of peak current densities at $+60$ mV. Bars represent the mean \pm SEM. $*p < 0.05$ vs. control cells ($n = 6$). QUE: quercetin.

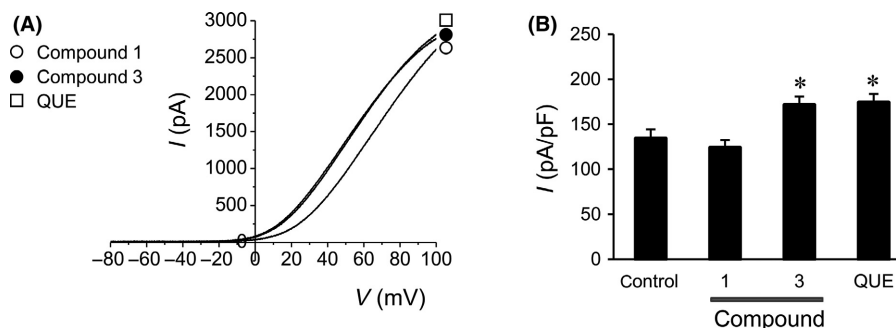
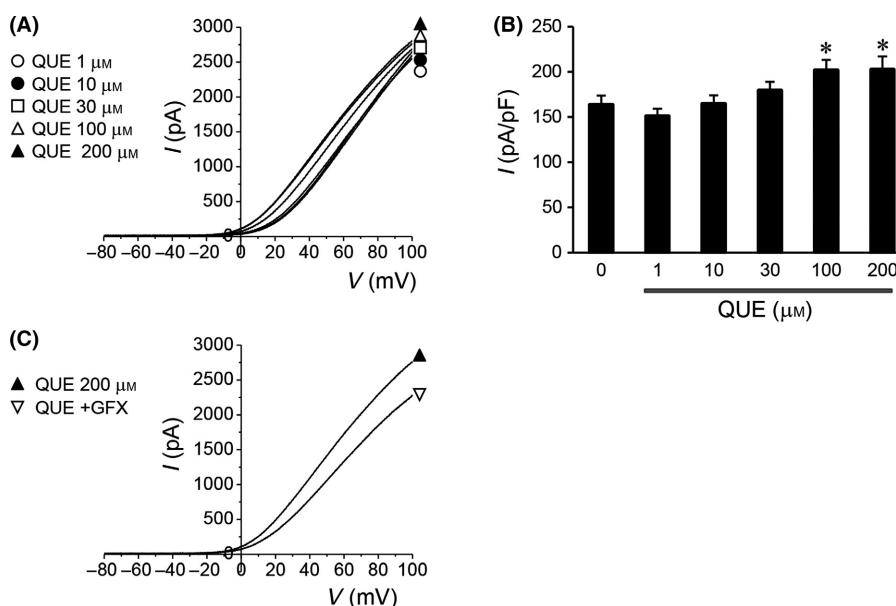


Figure 9 Concentration-dependent activation of Hv1 currents by quercetin. (A) Maximum current–voltage relationships were obtained before (control) and after the addition of various concentrations of quercetin. All currents were induced by a ramp protocol from -80 to $+100$ mV for 2 sec. Quercetin was applied at 1 – $200\ \mu\text{M}$ to Hv1-overexpressing HEK293 cells. $\text{pH}_i = 6.0$; $\text{pH}_o = 7.4$. (B) Summary of the dose-dependent increase in Hv1 current in response to the addition of quercetin at $+60$ mV. Bars represent the mean \pm SEM. $*p < 0.05$ vs. control cells ($0\ \mu\text{M}$) ($n = 10$). (C) Effect of GF109203X on quercetin-induced potentiation of Hv1 channel currents. Currents were recorded after the addition of $200\ \mu\text{M}$ quercetin (▲) and then in the presence of $3\ \mu\text{M}$ GF109203X (▼). QUE: quercetin.



resulting from the pro-oxidant effects of quercetin is of special interest because H_2O_2 plays important roles in cellular signaling via directly activating a specific isoform of PKC (Gopalakrishna & Jaken, 2000; Majumder *et al.*, 2001) and via the regulation of ion channels.

Furthermore, a recent report showed that H_2O_2 induces superoxide production, stimulating sperm motility in a NOX-5-dependent manner. Those authors demonstrated that superoxide production and enhanced sperm motility were pH dependent and that there was a functional interaction between the Hv1 channel and NOX-5 in human spermatozoa (Musset *et al.*, 2012). Limited amounts of ROS are known to play important roles in many sperm physiological processes, such as capacitation, the acrosome reaction, hyperactive motility, and oocyte fusion and fertilization (Decoursey, 2003; Aitken *et al.*, 2004). Thus, our results suggest that the pro-oxidant effects of quercetin play a significant role in the OPE-induced activation of the Hv1 channel.

The PKC family consists of serine/threonine kinases that mediate various cellular signaling responses. Moreover, PKC is a potent regulator of channel activity; specifically, the functional properties of ion channel proteins are commonly altered via phosphorylation. One study showed that PKC (PKC δ)-dependent phosphorylation of hHv1, specifically at Thr29, is responsible for converting the resting channel into the enhanced gating mode (Musset *et al.*, 2010). During the enhanced gating mode, the threshold voltage of activation shifts toward more negative potentials by approximately 40 mV, and the maximal H^+ conductance increases, whereas the Zn^{2+} sensitivity does not change. Consistent with the findings of our current study, several previous studies have reported that arachidonic acid and lipopolysaccharide affect Hv1 channel activities by modulating the gating mode through PKC (Morgan *et al.*, 2007; Szteyn *et al.*, 2012).

Many studies have demonstrated that quercetin modulates PKC activity in a cell type-specific and isoform-specific manner

(Zhang *et al.*, 2005; Bandyopadhyay *et al.*, 2008; Granado-Serrano *et al.*, 2008; Maurya & Vinayak, 2015). A recent study reported that quercetin upregulates PKC δ expression and promotes PKC δ activity in DL mice (Maurya & Vinayak, 2015). Although accumulating evidence indicates that OPE contributes to PKC signaling pathways, the direct mechanism underlying this contribution has not yet been elucidated.

Voltage-gated proton (Hv1) channels play important roles in various physiological and pathological processes. The best-characterized physiological functions of these channels are stabilizing NADPH oxidase activity during the phagocytic respiratory burst and compensating for membrane depolarization and intracellular acidification via Hv1-dependent H⁺ efflux. Recently, Hv1 proton channels were reported to play an important role in sperm capacitation and hypermotility, suggesting that these channels as an attractive drug target for controlling male fertility. Many studies have indicated that quercetin has beneficial effects on multiple sperm parameters, such as improving epididymal sperm quality and motility and decreasing the risk of degenerative diseases.

Herein, we found that quercetin-rich OPE potentiated Hv1 currents by altering the current activation kinetics of these channels. Moreover, OPE shifted the conductance–voltage (G–V) relationships of Hv1 channels in the negative direction. The activation time constant was also significantly decreased after OPE treatment. These effects indicate that OPE promotes channel opening by altering the voltage-dependent gating of the channel. To the best of our knowledge, this study is the first to demonstrate that OPE activates Hv1 channels. This finding suggests that, in addition to its antioxidant effects, OPE might exert a beneficial effect on male fertility in humans by modulating Hv1 channel activity. We also suggest that these effects are due to the quercetin content of OPE.

CONCLUSIONS

Our results indicate that OPE induces Hv1 channel potentiation by enhancing channel gating via PKC in human embryonic kidney cell line HEK293. We hypothesize that this mechanism underlies the beneficial properties of OPE on sperm motility. Therefore, these results might lead to the development of drugs that effectively target the Hv1 channel and could be used to treat male infertility.

ACKNOWLEDGEMENTS

This research was supported by a grant of the Korea Health Technology R&D Project through the Korea Health Industry Development Institute (KHIDI), funded by the Ministry of Health & Welfare, Republic of Korea (HI14C0018).

DISCLOSURES

The authors have no conflicts of interest or financial ties to disclose.

AUTHORS' CONTRIBUTIONS

MRC, BRC, and SWL conceived and designed the idea for the article. MRC, JKP, and SWL contributed to drafting the manuscript. MRC, SJK, BRC, CYK, and HKK acquired the data. MRC, HKK, BRC, CYK, JKP, KPL, and SWL analyzed and interpreted the

data. JKP, KPL, and SWL provided guidance and critically revised the article.

REFERENCES

- Aitken RJ, Ryan AL, Baker MA & McLaughlin EA. (2004) Redox activity associated with the maturation and capacitation of mammalian spermatozoa. *Free Radic Biol Med* 36, 994–1010.
- Bandyopadhyay S, Romero JR & Chattopadhyay N. (2008) Kaempferol and quercetin stimulate granulocyte-macrophage colony-stimulating factor secretion in human prostate cancer cells. *Mol Cell Endocrinol* 287, 57–64.
- Cherny VV & DeCoursey TE. (1999) pH-dependent inhibition of voltage-gated H(+) currents in rat alveolar epithelial cells by Zn(2+) and other divalent cations. *J Gen Physiol* 114, 819–838.
- DeCoursey TE. (1991) Hydrogen ion currents in rat alveolar epithelial cells. *Biophys J* 60, 1243–1253.
- Decoursey TE. (2003) Voltage-gated proton channels and other proton transfer pathways. *Physiol Rev* 83, 475–579.
- Farhi J & Ben-Haroush A. (2011) Distribution of causes of infertility in patients attending primary fertility clinics in Israel. *Isr Med Assoc J* 13, 51–54.
- Gopalakrishna R & Jaken S. (2000) Protein kinase C signaling and oxidative stress. *Free Radic Biol Med* 28, 1349–1361.
- Granado-Serrano AB, Angeles Martin M, Bravo L, Goya L & Ramos S. (2008) Time-course regulation of quercetin on cell survival/proliferation pathways in human hepatoma cells. *Mol Nutr Food Res* 52, 457–464.
- Hamada AJ, Montgomery B & Agarwal A. (2012) Male infertility: a critical review of pharmacologic management. *Expert Opin Pharmacother* 13, 2511–2531.
- Hille B. (1986) Ionic channels: molecular pores of excitable membranes. *Harvey Lect* 82, 47–69.
- Iovannisci D, Illek B & Fischer H. (2010) Function of the HVCN1 proton channel in airway epithelia and a naturally occurring mutation, M91T. *J Gen Physiol* 136, 35–46.
- Izawa H, Kohara M, Aizawa K, Suganuma H, Inakuma T, Watanabe G, Taya K & Sagai M. (2008) Alleviative effects of quercetin and onion on male reproductive toxicity induced by diesel exhaust particles. *Biosci Biotechnol Biochem* 72, 1235–1241.
- Jung JY, Lim Y, Moon MS, Kim JY & Kwon O. (2011) Onion peel extracts ameliorate hyperglycemia and insulin resistance in high fat diet/streptozotocin-induced diabetic rats. *Nutr Metab (Lond)* 8, 18.
- Khaki A, Fathiazad F, Nouri M, Khaki AA, Khamenahi HJ & Hamadeh M. (2009) Evaluation of androgenic activity of allium cepa on spermatogenesis in the rat. *Folia Morphol (Warsz)* 68, 45–51.
- Kim KA & Yim JE. (2015) Antioxidative activity of onion peel extract in obese women: a randomized, double-blind, placebo controlled study. *J Cancer Prev* 20, 202–207.
- Kirichok Y & Lishko PV. (2011) Rediscovering sperm ion channels with the patch-clamp technique. *Mol Hum Reprod* 17, 478–499.
- Kirichok Y, Navarro B & Clapham DE. (2006) Whole-cell patch-clamp measurements of spermatozoa reveal an alkaline-activated Ca²⁺ channel. *Nature* 439, 737–740.
- Koch HP, Kurokawa T, Okochi Y, Sasaki M, Okamura Y & Larsson HP. (2008) Multimeric nature of voltage-gated proton channels. *Proc Natl Acad Sci USA* 105, 9111–9116.
- Lanzotti V. (2006) The analysis of onion and garlic. *J Chromatogr A* 1112, 3–22.
- Lee SM, Moon J, Do HJ, Chung JH, Lee KH, Cha YJ & Shin MJ. (2012) Onion peel extract increases hepatic low-density lipoprotein receptor and ATP-binding cassette transporter A1 messenger RNA expressions in Sprague-Dawley rats fed a high-fat diet. *Nutr Res* 32, 210–217.
- Lishko PV, Botchkina IL, Fedorenko A & Kirichok Y. (2010) Acid extrusion from human spermatozoa is mediated by flagellar voltage-gated proton channel. *Cell* 140, 327–337.

- Lishko PV, Kirichok Y, Ren D, Navarro B, Chung JJ & Clapham DE. (2012) The control of male fertility by spermatozoan ion channels. *Annu Rev Physiol* 74, 453–475.
- Ly TN, Hazama C, Shimoyamada M, Ando H, Kato K & Yamauchi R. (2005) Antioxidative compounds from the outer scales of onion. *J Agric Food Chem* 53, 8183–8189.
- Majumder PK, Mishra NC, Sun X, Bharti A, Kharbanda S, Saxena S & Kufe D. (2001) Targeting of protein kinase C delta to mitochondria in the oxidative stress response. *Cell Growth Differ* 12, 465–470.
- Maurya AK & Vinayak M. (2015) Modulation of PKC signaling and induction of apoptosis through suppression of reactive oxygen species and tumor necrosis factor receptor 1 (TNFR1): key role of quercetin in cancer prevention. *Tumour Biol* 36, 8913–8924.
- Moon J, Do HJ, Kim OY & Shin MJ. (2013) Antiobesity effects of quercetin-rich onion peel extract on the differentiation of 3T3-L1 preadipocytes and the adipogenesis in high fat-fed rats. *Food Chem Toxicol* 58, 347–354.
- Morgan D, Cherny VV, Finnegan A, Bollinger J, Gelb MH & DeCoursey TE. (2007) Sustained activation of proton channels and NADPH oxidase in human eosinophils and murine granulocytes requires PKC but not cPLA2 alpha activity. *J Physiol* 579, 327–344.
- Musset B, Capasso M, Cherny VV, Morgan D, Bhamrah M, Dyer MJ & DeCoursey TE. (2010) Identification of Thr29 as a critical phosphorylation site that activates the human proton channel Hvcn1 in leukocytes. *J Biol Chem* 285, 5117–5121.
- Musset B, Clark RA, DeCoursey TE, Petheo GL, Geiszt M, Chen Y, Cornell JE, Eddy CA, Brzyski RG & El Jamali A. (2012) NOX5 in human spermatozoa: expression, function, and regulation. *J Biol Chem* 287, 9376–9388.
- Okochi Y, Sasaki M, Iwasaki H & Okamura Y. (2009) Voltage-gated proton channel is expressed on phagosomes. *Biochem Biophys Res Commun* 382, 274–279.
- Ola-Mudathir KF, Suru SM, Fafunso MA, Obioha UE & Faremi TY. (2008) Protective roles of onion and garlic extracts on cadmium-induced changes in sperm characteristics and testicular oxidative damage in rats. *Food Chem Toxicol* 46, 3604–3611.
- Platts AE, Dix DJ, Chemes HE, Thompson KE, Goodrich R, Rockett JC, Rawe VY, Quintana S, Diamond MP, Strader LF & Krawetz SA. (2007) Success and failure in human spermatogenesis as revealed by teratozoospermic RNAs. *Hum Mol Genet* 16, 763–773.
- Prochazkova D, Bousova I & Wilhelmova N. (2011) Antioxidant and prooxidant properties of flavonoids. *Fitoterapia* 82, 513–523.
- Ramsey IS, Ruchti E, Kaczmarek JS & Clapham DE. (2009) Hv1 proton channels are required for high-level NADPH oxidase-dependent superoxide production during the phagocyte respiratory burst. *Proc Natl Acad Sci USA* 106, 7642–7647.
- Saber TM, Abd El-Aziz RM & Ali HA. (2016) Quercetin mitigates fenitrothion-induced testicular toxicity in rats. *Andrologia* 48, 491–500.
- Szteyn K, Yang W, Schmid E, Lang F & Shumilina E. (2012) Lipopolysaccharide-sensitive H⁺ current in dendritic cells. *Am J Physiol Cell Physiol* 303, C204–C212.
- Wang Y, Li SJ, Wu X, Che Y & Li Q. (2012) Clinicopathological and biological significance of human voltage-gated proton channel Hv1 protein overexpression in breast cancer. *J Biol Chem* 287, 13877–13888.
- Yen GC, Duh PD, Tsai HL & Huang SL. (2003) Pro-oxidative properties of flavonoids in human lymphocytes. *Biosci Biotechnol Biochem* 67, 1215–1222.
- Zhang XM, Chen J, Xia YG & Xu Q. (2005) Apoptosis of murine melanoma B16-BL6 cells induced by quercetin targeting mitochondria, inhibiting expression of PKC-alpha and translocating PKC-delta. *Cancer Chemother Pharmacol* 55, 251–262.